JACS
JOURNAL OF THE AMERICAN CHEMICAL SOCIETY
pubs.acs.org/JACS
Communication

Contact with Electrically Conductive Inert Solids Alters Intrinsic Heterogeneous Brønsted Acid Catalysis

Bhavish Dinakar, Juan F. Torres, Mostapha Dakhchoune, Griffin Drake, Yogesh Surendranath, Mircea Dincă,* and Yuriy Román-Leshkov*

Cite This: https://doi.org/10.1021/jacs.5c12973
Read Online

ABSTRACT: Interfacial electric fields at heterogeneous catalyst surfaces have been demonstrated to alter kinetics of liquid-phase reactions. In these systems, electric fields are generated from applying a potential to the catalyst through connection to a potentiostat or through electron transfer from redox-active species in solution. Here, we demonstrate that catalyst polarization can also occur by simply contacting electrically conductive inert solids, leading to the counterintuitive conclusion that a catalyst particle touching an inert solid can alter intrinsic reaction rates. Using dehydration of 1-methylcyclopentanol to 1-methylcyclopentene catalyzed by Brønsted-acidic carboxylic acid groups on carbon nanotubes as a proof-of-concept probe reaction, we show that catalyst contact with inert, thermally reduced carbon nanotubes leads to order-of-magnitude changes in reaction rate. Furthermore, we demonstrate that these contact-induced effects can also be observed under standard laboratory reaction conditions, where particle-to-particle contact in stirred catalyst powder suspensions is sufficient to demote rates by ∼8-fold. This work provides the foundation for a new method of reaction rate control, which could have implications whenever heterogeneous catalyst particles are in contact with inert materials for liquid-phase reactions in the presence of electrolyte.

Applied potentials have emerged as a powerful handle to drive heterogeneously catalyzed liquid-phase chemical transformations.[1] Although traditionally used in electrocatalysis to drive product formation through electrochemical half-reactions,[2] applied potentials can also accelerate the rates of purely thermochemical reactions that involve no net electron transfer.[3,4] Such thermochemical promotion has been observed across diverse reactions, including olefin isomerization,[5] hydrazine and hydrogen oxidation,[6,7] carbon dioxide and ethylene hydrogenation,[8−11] epoxide isomerization,[12] alcohol dehydration,[8,13] and Friedel−Crafts acylation.[8] For these systems, the non-Faradaic promotion mechanism has been demonstrated by observing greater-than-unity Faradaic efficiencies, surpassing the purely electrochemical theoretical limit.[2]

We previously reported that alcohol dehydration rates, specifically converting 1-methylcyclpentanol (MCPol) to 1-methylcyclopentene (MCPene), are particularly sensitive to applied potential when catalyzed by electrically conductive heterogeneous Brønsted acid catalysts.[8,13] Catalyst systems explored include phosphotungstic acid supported on carbon black, acidic surface hydroxyls on Ti foil, and carboxylic acids on carbon black, carbon paper, and multiwalled carboxylic acid-functionalized carbon nanotubes (denoted COOH−CNTs).[8,13]

When a positive potential is applied to the catalyst immersed in an electrolyte solution, the catalyst accumulates positive charge, with charge-counterbalancing anions migrating to the catalyst/electrolyte interface.[2] The resulting charge separation generates a strong interfacial potential drop and corresponding electric field (Figure 1A).[14] This localized electric field destabilizes positively charged protons (H^+) bound to active sites via electrostatic repulsion, increasing their effective acidity.[8,13,15,16] Consequently, during the reaction cycle, positive polarization drives proton transfer from the active sites to MCPol, drastically increasing overall reaction rates.[8,13]

Because of this powerful electrostatic interaction, reaction rates show remarkably strong dependence on applied potential, with reaction rates increasing 10-fold for every 80−130 mV of applied potential, rivaling the potential dependencies found in Faradaic electrocatalysis (Figure 1B).[8,13] Specifically, for COOH−CNT catalysts, we developed a method to polarize catalyst powder by encasing the powder in a stainless steel mesh that served as a physical support and conductive electrode. Using this "basket electrode," we demonstrated that thermochemical reaction rates can be modulated across a dynamic range of 100,000-fold by varying the applied potential without changing active site density.[13]

Traditionally, two approaches have been utilized to polarize catalysts (Figure 1C). The first approach, "wired polarization," uses a potentiostat-connected working electrode (WE), which transfers charge from a counter electrode (CE) until the WE reaches the desired potential relative to a reference electrode (RE).[8,9,13] The second approach, or "wireless polarization," employs equilibrium redox couples (such as ferrocene/ferrocenium) dissolved in the reaction solution, wherein the

Received: July 29, 2025
Revised: November 4, 2025
Accepted: November 26, 2025

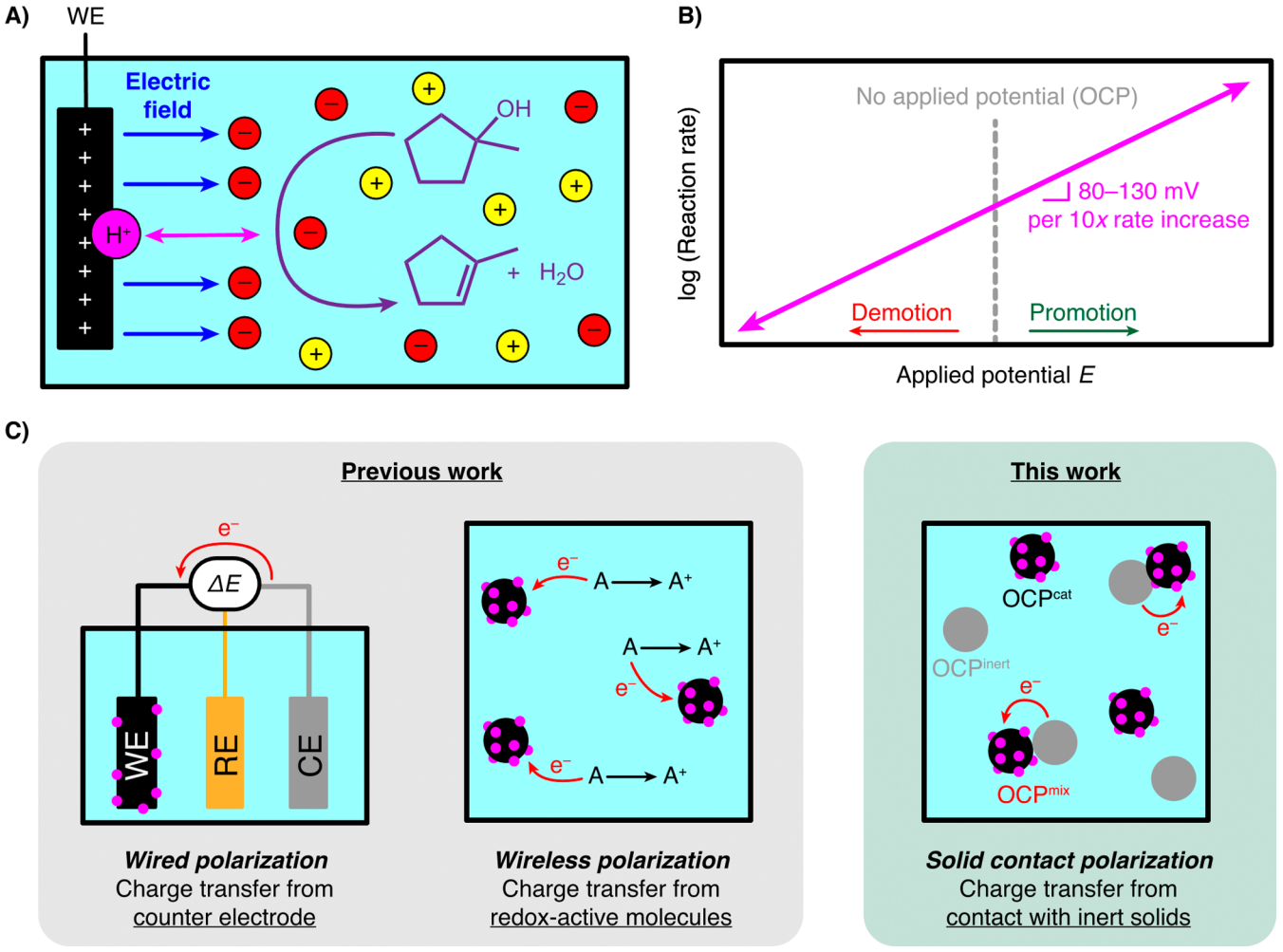

Figure 1. (A) Diagram of rate promotion of Brønsted acid-catalyzed MCPol dehydration in electrolyte solution in which the interfacial electric field repels the acidic H^+ from the working electrode (WE) to increase the effective acidity. The WE is charged by a counter electrode (CE) and maintained at constant potential relative to a reference electrode (RE). (B) Previously obtained rate-potential scalings for MCPol dehydration, in which rates can be promoted and demoted below open circuit potential. (C) Comparison of previous catalyst polarization methods with this work.

catalyst exchanges electrons with these species until reaching an equilibrium potential described by the Nernst equation.[8,9,17]

In both approaches, when a material i is polarized to a potential E^i, this potential corresponds to the difference in the electrochemical potential of electrons for material i relative to RE given by

$$E^i = -\frac{1}{F}(\hat{\mu}_e^i - \hat{\mu}_e^{RE}) \tag{1}$$

where $\hat{\mu}_e^i$ represents the electrochemical potential of the electrons in material i and F denotes Faraday's constant.[2] The electrochemical potential of electrons is related to the electrostatic potential by

$$\hat{\mu}_e^i = \mu_e^i - F\phi^i \tag{2}$$

where ϕ^i denotes the electrostatic potential of material i relative to a bulk solution reference state and μ_e^i denotes the electron chemical potential of material i.[2] Therefore, two different materials i and j which are both uncharged (and therefore have $\phi^i = \phi^j = 0$) may still have different electron chemical potentials ($\mu_e^i \neq \mu_e^j$). In the absence of substantial Faradaic reactivity, these differences in chemical potential will translate into distinct values of the catalyst open circuit potential (OCP), which refers to the electron electrochemical potential, E, in the absence of external polarization.[2]

We reasoned that there could be an alternative strategy to control catalyst polarization by contacting a catalyst with a defined OCP^{cat} with another electrically conductive, inert solid having a distinct OCP^{inert} such that $OCP^{cat} \neq OCP^{inert}$. Upon contact, electrons should spontaneously transfer from the lower-OCP material to the higher-OCP material until their potentials equilibrate to an intermediate value denoted OCP^{mix} (Figure 1C). The amount of charge ΔQ^i transferred during this process depends on the material's gravimetric specific capacitance C^i and the mass m^i by[18]

$$\Delta Q^i = C^i m^i \Delta E^i \tag{3}$$

Thus, for a catalyst initially at OCP^{cat} and an inert solid initially at OCP^{inert}, conservation of charge ($\Delta Q^{cat} = -\Delta Q^{inert}$) allows solving for OCP^{mix} (Supporting Information, Section S5.1) as

$$OCP^{mix} = \frac{OCP^{cat} + \left(\frac{C^{inert}}{C^{cat}}\right)\left(\frac{m^{inert}}{m^{cat}}\right)OCP^{inert}}{1 + \left(\frac{C^{inert}}{C^{cat}}\right)\left(\frac{m^{inert}}{m^{cat}}\right)} \tag{4}$$

https://doi.org/10.1021/jacs.5c12973
J. Am. Chem. Soc. XXXX, XXX, XXX−XXX

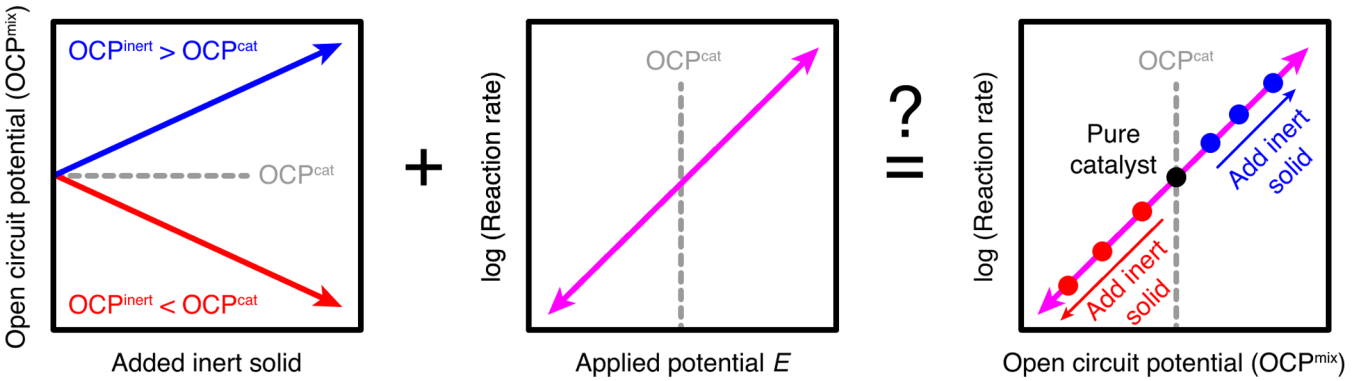

Figure 2. Hypothesized reaction rate change from catalyst contact with electrically conductive inert solid, which transfers charge to the catalyst due to difference in electron chemical potential and therefore alters the catalyst potential.

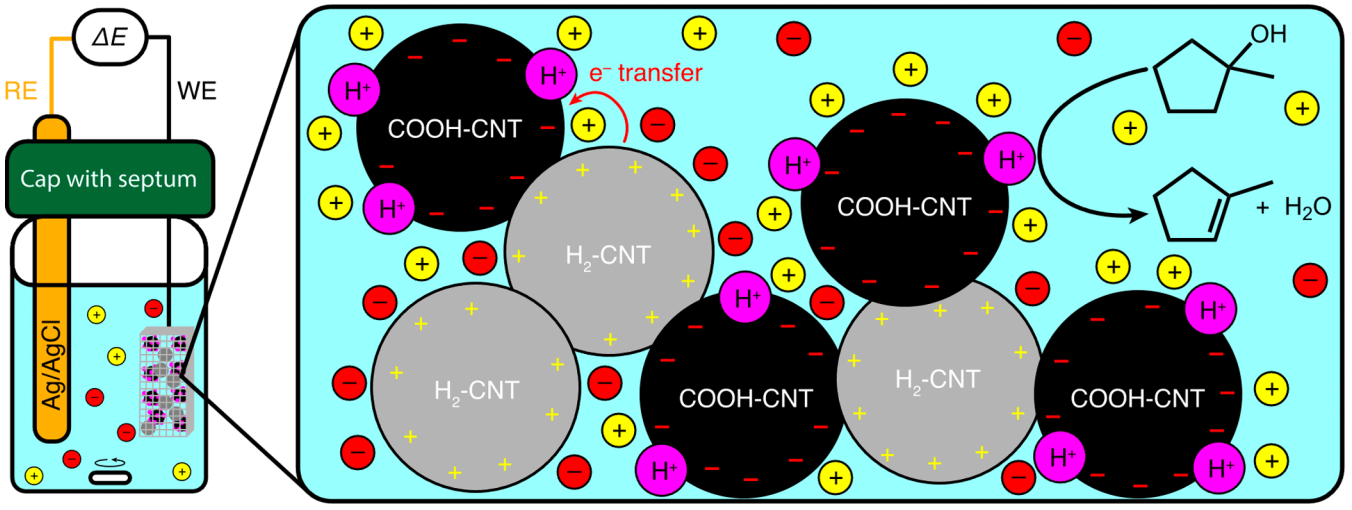

Figure 3. Diagram for experimental setup for measuring catalyst/inert contact effects on alcohol dehydration. The WE (COOH−CNT catalyst and H_2−CNT inert encased in a stainless steel mesh basket electrode) and RE (Ag/AgCl electrode) are immersed in the reaction solution in a stirred septum-capped 20 mL glass vial. The magnified inset depicts electron transfer from the H_2−CNT (gray) to COOH−CNT (black) due to their OCP difference, causing the catalyst (black) to gain negative charge relative to its charge state at its OCP. This charge transfer alters the local electric field at the Brønsted acid active sites and thereby modulates alcohol dehydration rates.

Hence, OCP^{mix} differs most significantly from OCP^{cat} when the OCPs mismatch and both the specific capacitance ratio C^{inert}/C^{cat} and mass ratio m^{inert}/m^{cat} are large. Importantly, these shifts, when coupled to the established rate-potential scaling, imply that seemingly inert solids can promote or demote reaction rates when in contact with conductive catalyst particles due purely to charge transfer between the materials.

Here, we demonstrate that contact-induced polarization provides a simple yet powerful means to modulate the rates of Brønsted acid-catalyzed alcohol dehydration via solid−solid electron equilibration (Figure 2). Using the dehydration of MCPol catalyzed by COOH−CNTs as a probe reaction, we show that contact with thermally reduced, inert carbon nanotubes causes order-of-magnitude rate suppression. Importantly, this effect persists under practical conditions: when COOH−CNT catalysts are stirred in liquid-phase suspensions, particle-to-particle collisions are sufficient to demote activity by an order of magnitude. These results reveal that inert solids (often overlooked in catalytic design) can play an active role in determining reaction rates in systems comprising conductive catalysts and electrolyte.

To test the hypothesis underlying contact-induced polarization, we sought to identify a suitable pair of electrically conductive catalyst and inert materials meeting the following criteria: (i) the Brønsted-acidic catalyst exhibits well-characterized rate-potential scaling and remains sufficiently active to enable kinetic measurements without external polarization (i.e., at OCP^{cat}), (ii) the inert material must not independently contribute to reactivity, (iii) OCP^{cat} and OCP^{inert} differ substantially to drive measurable charge transfer, and (iv) C^{inert} is comparable to or greater than C^{cat} such that the transferred charge suffices to alter OCP^{mix} from OCP^{cat}.

We selected multiwalled carboxylic acid-functionalized carbon nanotubes (COOH−CNTs) as the probe catalyst material for dehydrating MCPol to MCPene. We previously found that carboxylic acid groups on COOH−CNTs catalyze this transformation with a rate-potential scaling of 141 ± 6 mV per 10-fold rate increase, with rate promotion for $E^{cat} > OCP^{cat}$ and demotion for $E^{cat} < OCP^{cat}$.[13]

To generate a suitable electrically conductive inert material with high capacitance, we thermally reduced COOH−CNTs at 1025 °C for 6 h under 5% H_2/N_2 atmosphere, producing what we denote as H_2−CNTs. This treatment desorbs volatile impurities and removes carboxylic acid groups (Figure S2),[19−21] which we hypothesized would remove the low-energy electronic states associated with the oxygenated

https://doi.org/10.1021/jacs.5c12973
J. Am. Chem. Soc. XXXX, XXX, XXX−XXX

functionalities, decreasing OCP.[22] Control experiments confirmed no detectable reactivity from H_2−CNT under all reaction conditions used in this study.

To evaluate reaction kinetics under contact-induced polarization, we introduced both COOH−CNT and H_2−CNT into the same stainless steel mesh basket electrode, allowing the materials to be in electrical contact with each other, whose potential (OCP^{mix}) was monitored via potentiostat (Figure 3). Reaction conditions were chosen to match those used in our prior rate-potential studies (Figure 4A).[13]

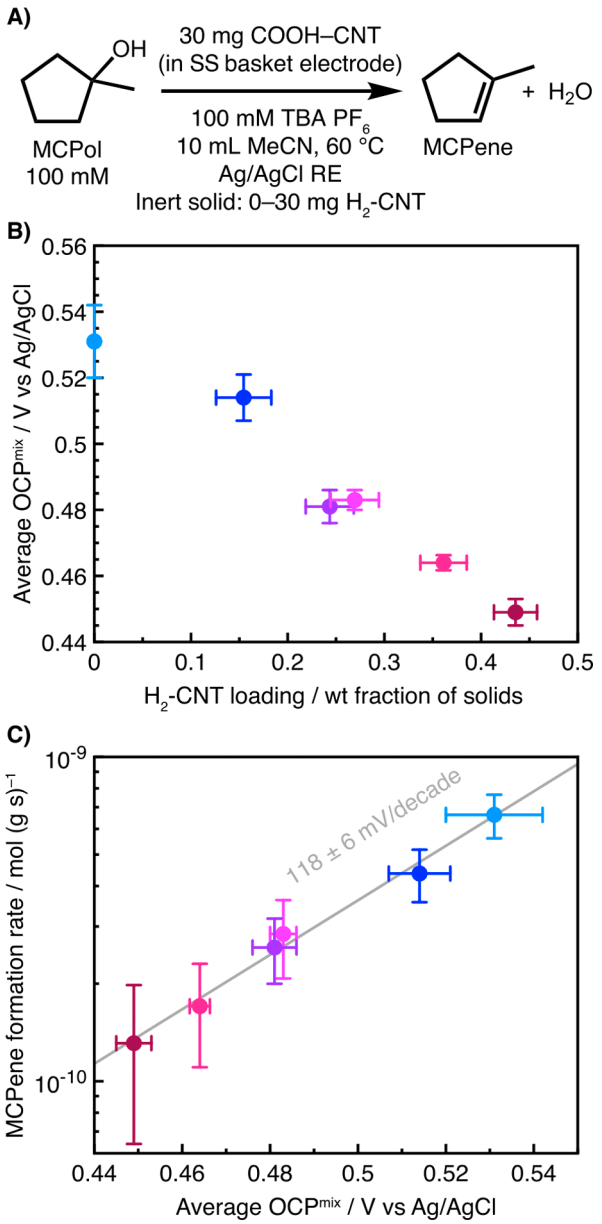

Figure 4. (A) Alcohol dehydration reaction conditions. (B) Dependence of average OCP^{mix} (measured *in situ*) on H_2−CNT loading (relative to COOH−CNT). *X*-axis error bars reflect propagated experimental uncertainties, and *Y*-axis error bars are standard deviations. (C) Log−linear dependence of MCPene formation rate (normalized to COOH−CNT mass) on average OCP^{mix}, altered by varying H_2−CNT loading. *X*-axis error bars are standard deviations, and *Y*-axis error bars reflect propagated experimental uncertainties.

We found the initial OCP^{cat} (measured immediately upon immersing the electrode into solution) to be ∼550 mV (vs Ag/AgCl RE) for COOH−CNT in the reaction solution (Figure S4). Contrastingly, we measured the initial OCP^{inert} of H_2−CNT to be ∼110 mV under the same conditions (Figure S10), consistent with a decrease in OCP upon reducing the COOH−CNTs. Therefore, we expected that adding H_2−CNTs to COOH−CNTs would cause electron transfer from the H_2−CNTs to the COOH−CNTs, negatively charging the COOH−CNT surface and lowering OCP^{mix} relative to OCP^{cat} (Figure 3).

As hypothesized, increasing H_2−CNT loading decreased the initial OCP^{mix} value (Figure S10). Additionally, the linear dependence of OCP^{mix} with H_2−CNT weight fraction aligns with our model predictions when $C^{inert} \approx C^{cat}$, demonstrating that the thermal treatment to generate H_2−CNT did not significantly alter its electrolyte-accessible surface area (Section S5). We note that OCP^{mix} drifts over time, likely due to redox-active impurities in the reaction solution[13] (Figure S4); nevertheless, the average OCP^{mix} (measured during the day-long reactions, and therefore the kinetically relevant OCP^{mix} value) also decreased similarly with H_2−CNT loading (Figure 4B).

Furthermore, we observed that increasing the H_2−CNT loading decreases the reaction rate because of the OCP change, yielding a log−linear dependence of rate on OCP (Figure 4C). The fitted rate-potential scaling of 118 ± 6 mV/decade is consistent with our previously observed scaling of 141 ± 6 mV/decade,[13] with slight discrepancies expected due to uncertainty in quantifying <0.1% product yields.

To rule out alternative explanations for rate suppression, such as changes in heat/mass transport, adsorption of reactant/product by inert solid, or active-site poisoning by leached species, we performed three key control experiments.

First, we measured reaction kinetics of the COOH−CNT/H_2−CNT basket system at a fixed potential of 0.6 V using a Ti foil CE. Under these externally controlled conditions, reaction rates were invariant with H_2−CNT loading (Figure 5A), indicating that the observed rate suppression requires open circuit polarization.

Second, we measured reaction kinetics under low-electrolyte conditions (0.1 mM TBA PF_6), which we previously demonstrated to diminish interfacial electric fields and attenuate rate-potential sensitivity. Under these conditions, varying the amount of H_2−CNT had no measurable effect on the reaction rate (Figure 5B), reinforcing that interfacial electric fields drive the observed rate modulation.

Third, we spatially separated 10 mg COOH−CNT and 20 mg H_2−CNT in two distinct basket electrodes immersed in the same reaction solution (100 mM TBA PF_6) without any other electrodes present. After 23 h at 80 °C, ^{1}H NMR analysis showed 0.1% product yield which although not very large (given the low acidity of COOH groups), is well above our detection threshold of ∼0.01% product yield. When we electrically connected the two basket electrodes outside the reaction solution with a wire under otherwise identical conditions, no product was detected. This result confirms that presence of electrical contact between catalyst and inert materials alone can determine whether the reaction proceeds.

Collectively, these control experiments confirm that the reaction rate is primarily governed by the open circuit potential of the catalyst, which in turn modulates the interfacial electric field strength and thereby alters the effective acidity of

https://doi.org/10.1021/jacs.5c12973
J. Am. Chem. Soc. XXXX, XXX, XXX−XXX

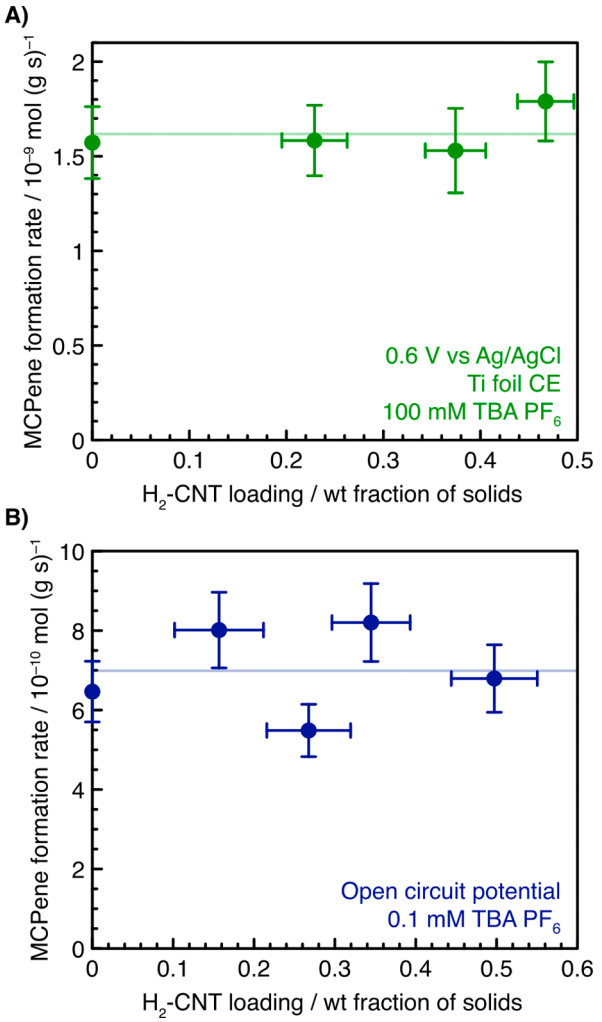

Figure 5. Invariance of MCPene formation rate (normalized to mass of COOH−CNT) with H_2−CNT loading (A) at a controlled potential of 0.6 V vs Ag/AgCl (B) with 0.1 mM TBA PF_6. Error bars reflect propagated experimental uncertainties.

Brønsted acid sites. The presence of conductive inert solids alters catalytic rates not through mass transfer limitations or poisoning, but through shifts in OCP that induce electrostatic changes at the active site analogous to external polarization with a potentiostat or electron transfer with redox mediators. However, the contact-induced method offers distinct advantages: it requires only the addition of an inert conductive solid, eliminating the need for counter electrodes and dissolved redox species. Moreover, the use of a solid-phase inert material avoids potential side reactions and facilitates straightforward separation from the reaction mixture.[8]

Finally, we hypothesized that the contact-induced polarization mechanism could manifest under standard laboratory conditions involving catalyst powder suspended in reaction solution, where particle−particle contact during stirring may induce the same charge transfer observed as the basket electrode setup.[23] To test this, we measured MCPol dehydration rates in stirred suspensions containing 10 mg COOH−CNT in 2 mL reaction solution, with and without adding 20 mg of H_2−CNT. In the presence of 100 mM TBA PF_6, adding H_2−CNT decreased the rate by ∼8-fold (Figure S7). However, like what we observed in the basket electrode, the observed rate was unaffected by the addition of H_2−CNT when the electrolyte concentration was reduced to 0.1 mM (Figure S8). These experiments confirm that rate suppression in the stirred system originates from contact-induced changes in catalyst potential.

Whereas contact-induced rate modulation has been reported in bifunctional catalytic systems, typically invoking local short-circuit[24−29] or spillover mechanisms[30] between two active sites that catalyze different steps or half reactions, our findings demonstrate that even contact between a single-function catalyst and a catalytically inert material can substantially modify the rate at the catalyst's own active sites. In both situations, the central variable that defines catalytic activity is its electrochemical potential, and factors that serve to alter this parameter will influence reaction rate.

Although our proof-of-concept study focuses on rate suppression for a particular reaction and catalyst/inert pair, enabled by the availability of well-characterized materials and favorable OCP alignment, we anticipate that the same framework could be employed to promote reaction rates for appropriately chosen catalyst-inert combinations. In particular, we expect rate promotion when $OCP^{inert} > OCP^{cat}$ for reaction classes with positively sloped rate-potential scalings. For reaction classes with negatively sloped rate-potential scalings, we expect rate promotion when $OCP^{inert} < OCP^{cat}$. Identification of suitable catalyst/inert materials and reaction classes could be aided by first-principles calculations that screen candidate materials for intrinsic acidity and chemical potential. The development of such systems remains an open challenge, and we encourage the community to explore this expanded space of electrostatically responsive catalyst design.

■ ASSOCIATED CONTENT

Supporting Information

The Supporting Information is available free of charge at https://pubs.acs.org/doi/10.1021/jacs.5c12973.

Materials and experimental methods, full characterization and experimental data, supplementary discussions (PDF)

Raw data (ZIP)

■ AUTHOR INFORMATION

Corresponding Authors

Yuriy Román-Leshkov − *Department of Chemical Engineering, Massachusetts Institute of Technology, Cambridge, Massachusetts 02139, United States;* orcid.org/0000-0002-0025-4233; Email: yroman@mit.edu

Mircea Dincă − *Department of Chemistry, Massachusetts Institute of Technology, Cambridge, Massachusetts 02139, United States;* orcid.org/0000-0002-1262-1264; Email: mdinca@mit.edu

Authors

Bhavish Dinakar − *Department of Chemical Engineering, Massachusetts Institute of Technology, Cambridge, Massachusetts 02139, United States;* orcid.org/0000-0002-7611-101X

Juan F. Torres − *Department of Chemistry, Massachusetts Institute of Technology, Cambridge, Massachusetts 02139, United States*

https://doi.org/10.1021/jacs.5c12973
J. Am. Chem. Soc. XXXX, XXX, XXX−XXX

Mostapha Dakhchoune − *Department of Chemical Engineering, Massachusetts Institute of Technology, Cambridge, Massachusetts 02139, United States*
Griffin Drake − *Department of Chemical Engineering, Massachusetts Institute of Technology, Cambridge, Massachusetts 02139, United States*
Yogesh Surendranath − *Department of Chemistry, Massachusetts Institute of Technology, Cambridge, Massachusetts 02139, United States;* orcid.org/0000-0003-1016-3420

Complete contact information is available at: https://pubs.acs.org/10.1021/jacs.5c12973

Notes

The authors declare no competing financial interest.

■ ACKNOWLEDGMENTS

This work was supported by the Department of Energy, Office of Basic Energy Sciences, where work in the Román Lab was supported under Award DE-SC0016214 and work in the Dincă Lab was supported under Award DE-SC0023288. B.D was supported by the National Science Foundation Graduate Research Fellowship Program (GRFP) under grant number 2141064. M.D. (Mostapha Dakhchoune) was supported by the Schmidt Science Fellowship. Nuclear magnetic resonance spectroscopy was performed at the MIT DCIF via the use of its shared user facilities. We thank Blake A. Johnson for helpful discussions.

■ REFERENCES

(1) Che, F.; Gray, J. T.; Ha, S.; Kruse, N.; Scott, S. L.; Mcewen, J.-S. Elucidating the Roles of Electric Fields in Catalysis: A Perspective. *ACS Catal.* **2018**, *8* (6), 5153−5174.
(2) Fuller, T. F.; Harb, J. N. *Electrochemical Engineering*; John Wiley & Sons: 2018.
(3) Vayenas, C. G.; Bebelis, S.; Pliangos, C.; Brosda, S.; Tsiplakides, D. *Electrochemical activation of catalysis: promotion, electrochemical promotion, and metal-support interactions*; Springer: 2001.
(4) Vayenas, C. G.; Koutsodontis, C. G. Non-Faradaic electrochemical activation of catalysis. *J. Chem. Phys.* **2008**, *128* (18), No. 182506.
(5) Ploense, L.; Salazar, M.; Gurau, B.; Smotkin, E. S. Proton Spillover Promoted Isomerization of n-Butylenes on Pd-Black Cathodes/Nafion 117. *J. Am. Chem. Soc.* **1997**, *119* (47), 11550−11551.
(6) Sanabria-Chinchilla, J.; Asazawa, K.; Sakamoto, T.; Yamada, K.; Tanaka, H.; Strasser, P. Noble Metal-Free Hydrazine Fuel Cell Catalysts: EPOC Effect in Competing Chemical and Electrochemical Reaction Pathways. *J. Am. Chem. Soc.* **2011**, *133* (14), 5425−5431.
(7) Neophytides, S. G.; Tsiplakides, D.; Stonehart, P.; Jaksic, M.; Vayenas, C. G. Non-Faradaic Electrochemical Modification of the Catalytic Activity of Pt for H_2 Oxidation in Aqueous Alkaline Media. *J. Phys. Chem.* **1996**, *100* (35), 14803−14814.
(8) Westendorff, K. S.; Hülsey, M. J.; Wesley, T. S.; Román-Leshkov, Y.; Surendranath, Y. Electrically driven proton transfer promotes Brønsted acid catalysis by orders of magnitude. *Science* **2024**, *383* (6684), 757−763.
(9) Wesley, T. S.; Román-Leshkov, Y.; Surendranath, Y. Spontaneous Electric Fields Play a Key Role in Thermochemical Catalysis at Metal−Liquid Interfaces. *ACS Cent. Sci.* **2021**, *7* (6), 1045−1055.
(10) Cai, F.; Gao, D.; Zhou, H.; Wang, G.; He, T.; Gong, H.; Miao, S.; Yang, F.; Wang, J.; Bao, X. Electrochemical promotion of catalysis over Pd nanoparticles for CO_2 reduction. *Chem. Sci.* **2017**, *8* (4), 2569−2573.
(11) Ryu, J.; Surendranath, Y. Polarization-Induced Local pH Swing Promotes Pd-Catalyzed CO_2 Hydrogenation. *J. Am. Chem. Soc.* **2020**, *142* (31), 13384−13390.
(12) Gorin, C. F.; Beh, E. S.; Kanan, M. W. An Electric Field−Induced Change in the Selectivity of a Metal Oxide−Catalyzed Epoxide Rearrangement. *J. Am. Chem. Soc.* **2012**, *134* (1), 186−189.
(13) Dinakar, B.; Westendorff, K. S.; Torres, J. F.; Dakhchoune, M.; Groenhout, K.; Ewell, N.; Surendranath, Y.; Dincă, M.; Román-Leshkov, Y. Elucidating Electric Field-Induced Rate Promotion of Brønsted Acid-Catalyzed Alcohol Dehydration. *J. Am. Chem. Soc.* **2025**, *147* (31), 27599−27610.
(14) Zhang, L.; Hu, X.; Wang, Z.; Sun, F.; Dorrell, D. G. A review of supercapacitor modeling, estimation, and applications: A control/management perspective. *Renewable and Sustainable Energy Reviews* **2018**, *81*, 1868−1878.
(15) Jackson, M. N.; Pegis, M. L.; Surendranath, Y. Graphite-Conjugated Acids Reveal a Molecular Framework for Proton-Coupled Electron Transfer at Electrode Surfaces. *ACS Cent. Sci.* **2019**, *5* (5), 831−841.
(16) Warburton, R. E.; Hutchison, P.; Jackson, M. N.; Pegis, M. L.; Surendranath, Y.; Hammes-Schiffer, S. Interfacial field-driven proton-coupled electron transfer at graphite-conjugated organic acids. *J. Am. Chem. Soc.* **2020**, *142* (49), 20855−20864.
(17) Cheng, G.; Zhang, W.; Jentys, A.; Ember, E. E.; Gutiérrez, O. Y.; Liu, Y.; Lercher, J. A., Importance of interface open circuit potential on aqueous hydrogenolytic reduction of benzyl alcohol over Pd/C. *Nat. Commun.* **2022**, *13* (1). DOI: 10.1038/s41467-022-35554-1
(18) Purcell, E. M.; Morin, D. J. *Electricity and magnetism*; Cambridge University Press: 2013.
(19) Krishnankutty, N.; Vannice, M. A. The Effect of Pretreatment on Pd/C Catalysts. *J. Catal.* **1995**, *155* (2), 327−335.
(20) Krishnankutty, N.; Vannice, M. A. The Effect of Pretreatment on Pd/C Catalysts. *J. Catal.* **1995**, *155* (2), 312−326.
(21) Rioux, R.; Vannice, M. Dehydrogenation of isopropyl alcohol on carbon-supported Pt and Cu−Pt catalysts. *J. Catal.* **2005**, *233* (1), 147−165.
(22) Chen, J.; Wang, M.; Liu, B.; Fan, Z.; Cui, K.; Kuang, Y. Platinum catalysts prepared with functional carbon nanotube defects and its improved catalytic performance for methanol oxidation. *J. Phys. Chem. B* **2006**, *110* (24), 11775−11779.
(23) Mourshed, M.; Niya, S. M. R.; Ojha, R.; Rosengarten, G.; Andrews, J.; Shabani, B. Carbon-based slurry electrodes for energy storage and power supply systems. *Energy Storage Materials* **2021**, *40*, 461−489.
(24) Huang, X.; Akdim, O.; Douthwaite, M.; Wang, K.; Zhao, L.; Lewis, R. J.; Pattisson, S.; Daniel, I. T.; Miedziak, P. J.; Shaw, G.; Morgan, D. J.; Althahban, S. M.; Davies, T. E.; He, Q.; Wang, F.; Fu, J.; Bethell, D.; McIntosh, S.; Kiely, C. J.; Hutchings, G. J. Au−Pd separation enhances bimetallic catalysis of alcohol oxidation. *Nature* **2022**, *603* (7900), 271−275.
(25) Zhao, L.; Akdim, O.; Huang, X.; Wang, K.; Douthwaite, M.; Pattisson, S.; Lewis, R. J.; Lin, R.; Yao, B.; Morgan, D. J.; Shaw, G.; He, Q.; Bethell, D.; McIntosh, S.; Kiely, C. J.; Hutchings, G. J. Insights into the Effect of Metal Ratio on Cooperative Redox Enhancement Effects over Au- and Pd-Mediated Alcohol Oxidation. *ACS Catal.* **2023**, *13* (5), 2892−2903.
(26) Daniel, I. T.; Zhao, L.; Bethell, D.; Douthwaite, M.; Pattisson, S.; Lewis, R. J.; Akdim, O.; Morgan, D. J.; McIntosh, S.; Hutchings, G. J. Kinetic analysis to describe Co-operative redox enhancement effects exhibited by bimetallic Au−Pd systems in aerobic oxidation. *Catalysis Science & Technology* **2023**, *13* (1), 47−55.
(27) Kim, B.; Daniel, I.; Douthwaite, M.; Pattisson, S.; Hutchings, G. J.; McIntosh, S. Tafel Analysis Predicts Cooperative Redox Enhancement Effects in Thermocatalytic Alcohol Dehydrogenation. *ACS Catal.* **2024**, *14* (11), 8488−8493.
(28) Lodaya, K. M.; Tang, B. Y.; Bisbey, R. P.; Weng, S.; Westendorff, K. S.; Toh, W. L.; Ryu, J.; Román-Leshkov, Y.; Surendranath, Y. An electrochemical approach for designing

thermochemical bimetallic nitrate hydrogenation catalysts. *Nature Catalysis* **2024**, *7* (3), 262−272.
(29) Harraz, D. M.; Lodaya, K. M.; Tang, B. Y.; Surendranath, Y. Homogeneous-heterogeneous bifunctionality in Pd-catalyzed vinyl acetate synthesis. *Science* **2025**, *388* (6742), No. eads7913.
(30) Li, X.; Zhao, L.; Douthwaite, M.; Wang, K.; Akdim, O.; Daniel, I. T.; Oh, R.; Liu, L.; Wang, Z.; Meng, F.; Pattisson, S.; López-Martin, A.; Yang, J.; Huang, X. J.; Lewis, R. J.; Hutchings, G. J. Solvent-Free Benzyl Alcohol Oxidation Using Spatially Separated Carbon-Supported Au and Pd Nanoparticles. *ACS Catal.* **2024**, *14* (22), 16551−16561.

https://doi.org/10.1021/jacs.5c12973
J. Am. Chem. Soc. XXXX, XXX, XXX−XXX